mathematics

MDPI

Article

Simulation of MCDM Process—Stope and Fan Pattern Selection in an Underground Mine with Uncertainty

Katarina Urošević *, Zoran Gligorić, Ivan Janković, Branko Gluščević and Čedomir Beljić

Faculty of Mining and Geology, University of Belgrade, 11000 Belgrade, Serbia; zoran.gligoric@rgf.bg.ac.rs (Z.G.); ivan.jankovic@rgf.bg.ac.rs (I.J.); branko.gluscevic@rgf.bg.ac.rs (B.G.); cedomir.beljic@rgf.bg.ac.rs (Č.B.)
* Correspondence: katarina.urosevic@rgf.bg.ac.rs

Abstract: Multi-criteria decision making (MCDM) refers to methods and processes used to evaluate and prioritize options when multiple criteria are involved. Extensive research conducted in the past has shown that uncertainty is a pervasive challenge in the decision-making process, particularly in complex and dynamic environments, such as mining. When making decisions under uncertainty, especially in stope and fan pattern selection for underground mining, it is crucial to consider various aspects, including economic and production factors. This paper presents an application of simulation combined with the ranking alternatives by perimeter similarity (RAPS) method for optimal stope and fan pattern selection in an underground mine. The results obtained were compared with existing MCDM methodology technique for order of preference by similarity to ideal solution (TOPSIS) and showed a very high correlation, which indicates the applicability of new methodology for decision making in mining industry problems.

Keywords: decision making; simulation; mining industry; underground mine; stope selection; uncertainty; drilling and blasting

MSC: 90B50



Academic Editor: José Niño-Mora

Received: 13 February 2025
Revised: 21 February 2025
Accepted: 25 February 2025
Published: 27 February 2025

Citation: Urošević, K.; Gligorić, Z.; Janković, I.; Gluščević, B.; Beljić, Č. Simulation of MCDM Process—Stope and Fan Pattern Selection in an Underground Mine with Uncertainty. *Mathematics* **2025**, *13*, 786. https://doi.org/10.3390/math13050786

Copyright: © 2025 by the authors. Licensee MDPI, Basel, Switzerland. This article is an open access article distributed under the terms and conditions of the Creative Commons Attribution (CC BY) license (https://creativecommons.org/licenses/by/4.0/).

1. Introduction

Multi-criteria decision-making (MCDM) has proven to be an important approach in engineering, where decisions often involve multiple criteria with different dimensions. MCDM techniques enable engineers to systematically evaluate and prioritize alternatives based on numerous factors, helping in decision-making [1]. The history of MCDM methods reflects the evolution of decision theory and quantitative analysis over decades.

The development of MCDM methods is closely tied to the broader application of operations research tools. While the foundational concepts of MCDM can be traced back earlier, many widely used methods today—such as PROMETHEE [2], ELECTRE [3], AHP [4], and TOPSIS [5]—were developed primarily in the latter half of the 20th century, alongside numerous other similar approaches. Nowadays, we are seeing the creation of new multi-criteria optimization methods, the improvement of existing ones, and the development of various kinds of hybrid models. Adapting an existing method or creating a new one is a quite common activity when there is a problem that needs to be solved.

The presence of MCDM methods in mining engineering is common, according to Pouresmaieli et al. [6]. Numerous articles have been published in the last two decades, where successful application of MCDM has been proven.

Mining projects involve various activities necessary to produce the final product. Among these activities are drilling and blasting, which are closely linked. Together, they

serve the purpose of breaking rock away from larger masses or for further crushing rock materials. These two operations are almost inevitable in every mining project, even when it is about surface or underground ways of exploiting raw materials. The determination of the optimal blast geometry is important for achieving the intended outcomes in a fan (ring) blasting operation. To compute these parameters, researchers have created a range of empirical, numerical, and statistical models [7].

MCDM methods have become increasingly valuable in optimizing various aspects of underground mining, including blasting design, equipment selection, and overall mine planning. MCDM techniques are particularly useful in complex environments, like underground mines, where decisions often involve balancing multiple criteria, such as cost, safety, environmental impact, and operational efficiency.

Many authors have conducted their research by applying MCDM methods to solve complex problems in an underground mine, such as the selection of an adequate mining method [8], determining the best shaft location [9], mining access selection [10], and selection of optimal drilling and blasting patterns [11]. For stope layout optimization, researchers have applied different approaches, such as heuristic algorithms [12].

Li et al. [13] introduced a new CRITIC-GRA model to develop a multi-factor quantitative optimization for stope dimensions, enabling a thorough analysis with predefined safety and economic indicators. Another study that optimizes stope dimensions to achieve safe working conditions was presented by Qiu et al. [14]. An Ansys 19.2 numerical simulation was used to optimize stope structural parameters.

Onederra and Chitombo [15] proposed a design method for underground ring blasting that ensures engineers follow a systematic blast design approach, integrating traditional guidelines with advanced 3D/4D analysis, damage models, and simulations. It emphasizes risk identification, mitigation, and iterative design reviews as mining conditions change.

Wang et al. [16] optimized a design scheme for ring blasting. In their research, a new optimization method based on the Scaled Heelan (SH) model [17] is proposed to reduce brow damage, over-crushing, and bulking in ring blasting. The method improves hole arrangement and fragment size prediction. A case study at a copper mine showed a reduction in brow damage from 36.7% to 16.7% and an 11.3% improvement in loading efficiency. For example, Bai et al. [18] in their research presented an algorithm that optimizes sublevel stope design using cylindrical coordinates and geotechnical constraints. It determines the optimal stope and raise location through maximum flow optimization, producing realistic results for engineering use.

Vishwakarma et al. [19,20] optimized the burden to achieve the optimal ring blasting pattern. In their first study, they utilized an explicit dynamic-based modeler from M/s Ansys to optimize the burden in an underground hard rock mine. The simulation process was conducted for three holes with depths ranging from 14 to 14.5 m. Blasting pattern parameters and ground vibrations were also measured. The results of the study showed variations in the burden value range for getting a greater volume of rock along the free face under established conditions. In another study, they developed an empirical equation based on their numerical model. The study showed that the simulation-based prediction deviated by less than 15% from the experimental results.

Earlier research on the optimization of fan blasting patterns and stope optimization in underground mining has significantly contributed to the understanding and improvement of blasting practices. Studies have focused on various aspects of blast design, aiming to control ground vibrations, reduce overbreak, lower the costs, etc.

Numerous authors have made significant contributions to the field of fan blasting optimization in underground mining, achieving notable advancements in both theoretical and practical aspects of the discipline.

This paper provides an upgrade of an existing MCDM method. The novel RAPS [21] method has already been developed and applied as a tool to support the decision-making process in the mining industry, where efficient resource management and safety are crucial. The aim of this research is to evaluate its stability under conditions of uncertainty in input parameters. Through this research, the intention is to assess how reliable and efficient the method is in real, dynamic conditions, to ensure its further application in decision-making optimization in the mining industry.

This method consists of two stages. In the first stage, it involves normalization, weighting, and calculating the "magnitude" of a component to identify the optimal alternative and decompose the alternatives. The second stage applies the concept of perimeter similarity to setting up the ranking of the alternatives [21]. For upgrading this method, because of the uncertainty aspect of treating mining problems, simulation is implemented in the method.

In this research, how to select optimal stope parameters and optimal blasting patterns through mathematical assessment and simulation is presented. It involves the calculation of nine distinct fan patterns. One of the optimized parameters is stope height, with three different height values considered in the calculations. Another key parameter for optimization is burden, which is the distance between the ring plane and the nearest free face where rock is being blasted [15]. By combining three different burden values with three different stope heights, a total of nine fan patterns were generated. These nine alternatives are then compared based on the defined criteria. In this study, five criteria have been chosen to guide the selection of the best alternative to achieve the desired objectives.

There are many aims that are important to accomplish by applying an optimal blasting pattern. One of the criteria proposed for evaluation is the compactness index [22] of the fan blasting pattern, which depends on the area and perimeter of the shape that the proposed fan blasting pattern takes. This criterion means that the energy is concentrated more, enhancing the explosion's efficiency in transferring energy to the rock mass [23]. Another important aim to achieve in mining processes is to obtain adequate tonnage of the rock mass form for blasting operations, which can provide a planned capacity for the mining process. This criterion is difficult to calculate as a crisp value because of the nature of explosions. This is the reason why simulation is proposed because it allows us to capture the uncertainty related to the explosion line of a blasted rock mass. The third criterion that is considered as important in this research is the costs of each alternative. Managing drilling and blasting costs is important for maintaining profitability in small-scale underground mines, as these operations typically represent a significant portion of total expenses. Reducing these costs involves balancing efficiency and resource usage to ensure that mining remains both sustainable and financially viable. Costs are influenced by market factors, such as the prices of explosives, drill fuel, consumables, labor, and other related items. Another important criterion is drilling time because minimizing the time spent on this improves operational efficiency and increases overall productivity. Like the second criterion, this one can also be simulated to achieve more precise results, as it is difficult to ensure consistent drilling times for each drillhole, much less for the entire fan pattern. The uncertainty of this parameter stems from varying work environment conditions, equipment, operational factors, and labor force. Uncertainty related to the drilling time duration is quantified through the simulation process. The fifth criterion that is considered important for this selection process is achieving the desired fragmentation of the blasted rock mass. The importance of this aim is because of the practical issues concerning the next operations: loading of the mined mass, transportation, and milling [24].

The results obtained for the decision-making RAPS process combined with simulation were tested using an existing methodology. A validity test was conducted using simulation

and the MCDM method (TOPSIS), and the results are presented in the corresponding section of this paper.

2. Model of Stope and Fan Pattern Selection

2.1. Methodology of Ranking Alternatives by Perimeter Similarity (RAPS)

A decision-making matrix is a tool designed to assess and prioritize options according to a specific set of criteria. It helps structure and evaluate choices, leading to more informed decisions. In this context, there are defined sets of alternatives to choose from, along with criteria that determine how these alternatives are ranked. Each criterion should have either a minimum or maximum value, depending on which proper methods can provide a suitable solution. In this paper, the RAPS method is used for decision making in our underground mine problem. This method has been upgraded by applying simulation for some of the criteria that are not strictly defined and are better suited for simulation rather than being determined as a single fixed value.

To set this task, it is necessary to create the decision-making matrix in the following manner:

$$M = \left[x_{ij}\right]_{m\times n} = \begin{bmatrix} A/C & C_1 & C_2 & \dots & C_n \\ A_1 & x_{11} & x_{12} & \dots & x_{1j} \\ A_2 & x_{21} & x_{22} & \dots & x_{2j} \\ \vdots & \vdots & \vdots & \ddots & \vdots \\ A_m & x_{m1} & x_{m2} & \dots & x_{mn} \end{bmatrix} \quad (1)$$

where:

$A = [A_1, A_2, \dots, A_m]$—a given set of alternatives, where m is the total number of alternatives,

$C = [C_1, C_2, \dots, C_n]$—a given set of criteria, where n is the total number of criteria,

$\left[x_{ij}\right]_{m\times n}$—an assessment of alternative A_i with respect to a set of criteria.

In the steps below, how the problem of alternative ranking is solved is shown:

Step 1: Normalization of input data

Each criterion is associated with its own dimension, highlighting the multidimensional nature of the problem. This makes decision-making more difficult. To simplify the process, it is necessary to convert the multidimensional space into a dimensionless decision space. For criteria focused on benefits (max), a specific normalization technique is employed:

$$r_{ij} = \frac{x_{ij}}{max_i\left(x_{ij}\right)}, \quad \forall i \in [1,2,3\dots,m] \wedge j \in S_{benefit} \quad (2)$$

while for the cost (min) criteria:

$$r_{ij} = \frac{min_i\left(x_{ij}\right)}{x_{ij}}, \quad \forall i \in [1,2,3\dots,m] \wedge j \in S_{cost} \quad (3)$$

where:

$S_{benefit}$—a set of benefit criteria,
S_{cost}—a set of cost criteria.

The outcome of this normalization process is the normalized decision matrix:

$$(M) = [r_{ij}]_{m\times n} = \begin{bmatrix} A/C & C_1 & C_2 & \dots & C_n \\ A_1 & r_{11} & r_{12} & \dots & r_{1j} \\ A_2 & r_{21} & r_{22} & \dots & r_{2j} \\ \vdots & \vdots & \vdots & \ddots & \vdots \\ A_m & r_{m1} & r_{m2} & \dots & r_{mn} \end{bmatrix} \quad (4)$$

Step 2: Weighted normalization

For each normalized assessment r_{ij} do the weighted normalization as follows:

$$u_{ij} = w_j r_{ij},\ \forall i \in [1,2,3\dots,m],\ \forall j \in [1,2,3\dots,n] \quad (5)$$

The result of the weighted normalization process is the weighted normalized matrix.

$$U = [u_{ij}]_{m\times n} = \begin{bmatrix} A/C & C_1 & C_2 & \dots & C_n \\ A_1 & u_{11} & u_{12} & \dots & u_{1j} \\ A_2 & u_{21} & u_{22} & \dots & u_{2j} \\ \vdots & \vdots & \vdots & \ddots & \vdots \\ A_m & u_{m1} & u_{m2} & \dots & u_{mn} \end{bmatrix} \quad (6)$$

The standard deviation [25] is used to assign the weights of criteria and reduce subjectivity.

$$W = [w_1, w_2, ..., w_j] = \left[\frac{\sigma_1}{\sum_{j=1}^{n} \sigma_j} \frac{\sigma_2}{\sum_{j=1}^{n} d_j} ... \frac{\sigma_j}{\sum_{j=1}^{n} d_j} \right] \quad (7)$$

σ_j is the standard deviation of the normalized matrix shown in Equation (4).

To verify the accuracy of the criteria weight assignments, it is sufficient to sum all the weights; this total must equal 1.

$$\sum_{j=1}^{n} w_j = 1 \quad (8)$$

Step 3: Optimal alternative determination

Each element of the optimal alternative is determined as follows:

$$q_j = max\left(u_{ij} \middle| 1 \le j \le n\right), \forall i \in [1,2,3,\dots,m] \quad (9)$$

Optimal alternative is represented by the following set:

$$Q = \left\{q_1, q_2, q_3, \dots, q_j\right\},\ j = 1,\ 2,\ 3\dots,n \quad (10)$$

Step 4: Decomposition of the optimal alternative

This step involves decomposing the optimal alternative into two subsets or components. The Q set can be represented as the union of these two subsets:

$$Q = Q^{benefit} \cup Q^{cost} \quad (11)$$

If k is the total number of benefit criteria, then l=n−k is the total number of cost criteria. Hence, the optimal alternative is defined as:

$$Q = \{q_1, q_2, q_3 \dots, q_k\} \cup \{q_1, q_2, q_3 \dots, q_l\} \quad (12)$$

Step 5: Decomposition of the alternative

Similar to Step 4, we perform decomposition of each alternative:

$$Y_i = U_i^{benefit} \cup U_i^{cost}, \ \forall i \in [1, 2, 3 \ldots, m] \tag{13}$$

$$U_i = \{u_{i1}, u, u_{i3} \ldots, u_{ik}\} \cup \{u_{i1}, u_{i2}, u_{i3} \ldots, u_{ih}\}, \ \forall i \in [1, 2, 3 \ldots, m] \tag{14}$$

Step 6: Magnitude of the component

The magnitude for each component of the optimal alternative is calculated as defined by:

$$Q_k = \sqrt{q_1^2 + q_2^2 + q_3^2 \ldots + q_k^2} \tag{15}$$

$$Q_h = \sqrt{q_1^2 + q_2^2 + q_3^2 \ldots + q_h^2} \tag{16}$$

For each alternative, the same approach can be applied:

$$U_{ik} = \sqrt{u_{i1}^2 + u_{i2}^2 + u_{i3}^2 \ldots + u_{ik}^2}, \ \forall i \in [1, 2, 3.., m] \tag{17}$$

$$U_{ih} = \sqrt{u_{i1}^2 + u_{i2}^2 + u_{i3}^2 \ldots + u_{ih}^2}, \ \forall i \in [1, 2, 3.., m] \tag{18}$$

In the next step, the method is illustrated to show how it ranks the alternatives. This method relies on the similarity between the perimeter of the optimal alternative and that of the other alternatives.

Step 7: Ranking the alternatives by perimeter similarity (RAPS)

The perimeter of the optimal alternative is shown as the perimeter of the right angle triangle. Components Q_k and Q_h represent the base and the perpendicular side of the triangle, in that order:

$$P = Q_k + Q_h + \sqrt{Q_k^2 + Q_k^2} \tag{19}$$

The perimeter for each alternative is determined using the same method:

$$P_i = U_{ik} + U_{ih} + \sqrt{U_{ik}^2 + U_{ih}^2} \tag{20}$$

Perimeter similarity is defined as the ratio between the perimeter of each alternative and that of the optimal alternative:

$$PS_i = \frac{P_i}{P}, \ \forall i \in [1, 2, 3 \ldots, m] \tag{21}$$

The alternatives are now arranged in descending order based on PS_i.

Figure 1 shows the flow chart of the process for working the RAPS method, described above.

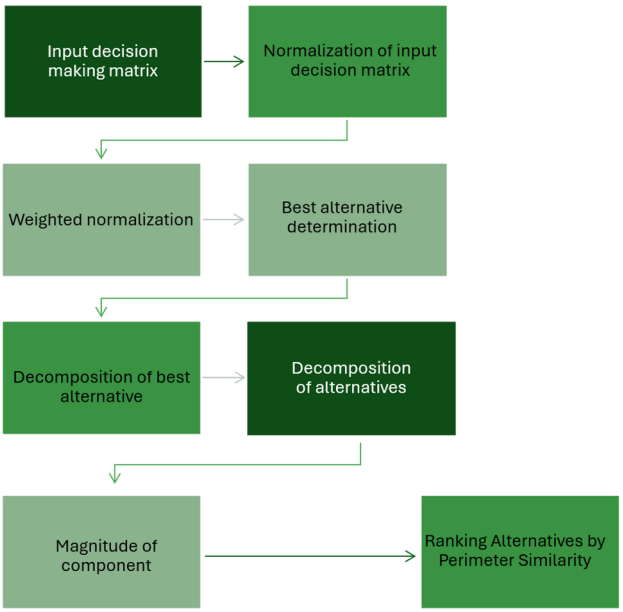


Figure 1. Flow chart of the RAPS method.

2.2. Simulation of the Selection Process

To determine the optimal parameters of the stope and blasting pattern, there are many aspects to consider for providing the required production capacity and optimal working conditions. In this paper, how to simultaneously select an optimal stope and fan pattern in an underground mine where exploitation of Bauxite is conducted is shown. The extraction of ore from rock mass is conducted through fan drilling and blasting. Fan blasting is important for the efficiency of ore extraction, influencing the fragmentation quality, and the overall stability of the underground mine. The research focuses on optimizing the height of the stope and key blasting parameters for selecting the best alternative to achieve better productivity. By employing a combination of MCDM, numerical simulations, empirical experience, and analysis, the study shows the optimal configurations for enhancing ore recovery while maintaining optimal time and minimizing costs. The paper concludes by presenting practical recommendations for the application of these optimization techniques in diverse underground mining situations, especially for small-scale mines.

In Figure 2, an example of a fan blasting pattern is shown where:

- H is the height of stope,
- h is width of the stope,
- x_b and y_b represents drilling limits for blastholes,
- w_d and h_d are dimensions of production drift, and
- b is burden.

Because of safety and to obtain the cleanest possible ore, meaning minimal dilution, a protective roof of one meter thickness is left intact and is not blasted and 0.8 m on the right side of the stope.

In this research, nine different fan patterns are calculated. The height of the stope (H in Figure 2) is one of parameters that is optimized. In this case, there are three different values of height that are entered into calculation. Another important parameter considered for optimization is burden ("b" value shown in Figure 2, cross section B-B'). Burden refers to the distance between the ring plane and the nearest free face where the rock volume is being blasted [15]. Combining three different values of burden and three different values of height of stope, nine fan patterns are gathered, and they represent our nine alternatives, which are compared with criteria described in the next paragraphs.

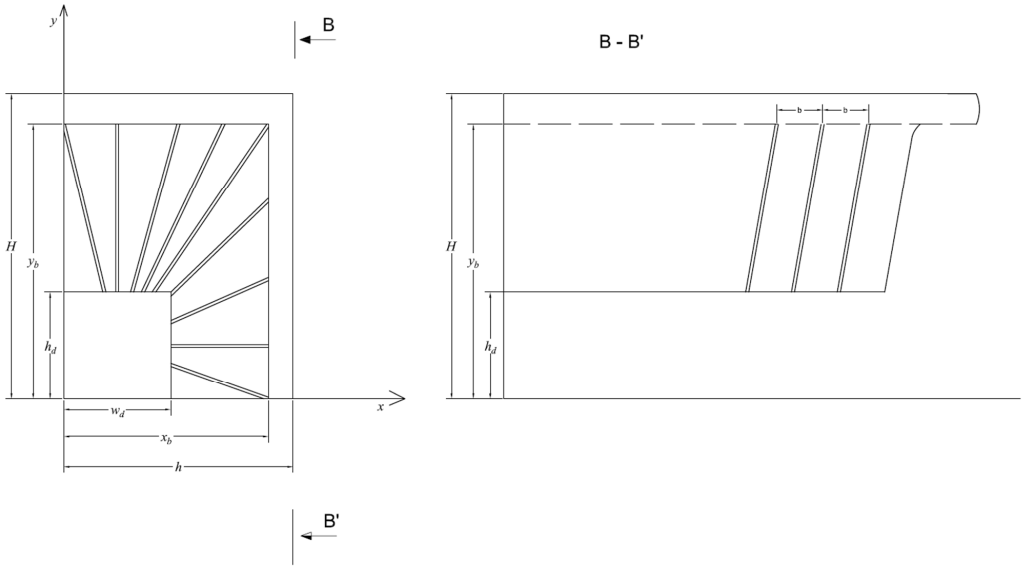


Figure 2. Fan blasting pattern.

To achieve the desired aims, five criteria were selected to guide the process of choosing the best alternative. The first criterion, C1, is the compactness index [22], and it is defined as the ratio of the square perimeter of the shape to the area covered by blastholes of the fan blasting pattern. The compactness index is defined as tending to the minimum. This means that the energy is more concentrated, making the explosion more efficient at transferring energy to the rock mass [23].

The equation for calculating compactness is:

$$C = \frac{P^2}{S} \tag{22}$$

where:

C—compactness,
S—surface of figure, which is defined by blastholes of fan pattern, m^2,
P—perimeter of figure, which is defined by blastholes of fan pattern, m.

$$C_i = |16 - C| \tag{23}$$

A compactness value of 16 is obtained from the ratio of the perimeter and area of a square, to which the compactness of the fans, in our example, also tends.

The next criterion, C2, that is considered in this research is tonnage. Tonnage is obtained as the product of the height and width of the stope, the adopted burden (b) and the bulk density of mined ore. The quantity of the mined ore is calculated as follows:

$$O = (x \cdot y - w_d \cdot h_d) \cdot b \cdot \gamma \tag{24}$$

where:

x—is width of explosion line, m,
y—is height of the explosion line, m,
w_d—width of production drift, m,
h_d—height of production drift, m,
b—burden, m,
γ—bulk density of mined ore, $\frac{t}{m^3}$.

Product "xy" represents the mined area, while product "$w_d h_d$" represents the area of production drift. We implemented a simulation approach to define the position of the explosion line along the x and y axes separately. The position of the line along the x-axis is x∈(x_b, h). One possible position can be defined by the following equation:

$$x = x_b + \Delta x \tag{25}$$

where Δx is governed by the normal distribution of the following form:

$$\Delta x \sim N(\mu, \sigma) \tag{26}$$

The parameter μ is the expectation of the distribution, and it is defined as follows:

$$\mu = \frac{x_b + h}{2} \tag{27}$$

The standard deviation of the distribution can be defined by the following equation:

$$\sigma = k \cdot (h - x_b) \tag{28}$$

where k is the coefficient, which takes the values of $0 \leq k \leq 0.5$.

The simulation approach enables us to capture uncertainty related to the position of the explosion line along the x-axis. The same approach is applied to the position of explosion line along the y-axis, and the simulation equation is presented as follows:

$$y = y_b + \Delta y = y_b + N(\frac{y_b + H}{2},\ k \cdot (H - y_b)) \tag{29}$$

A graph of the one possible position along the x and y axes is presented in Figure 3.

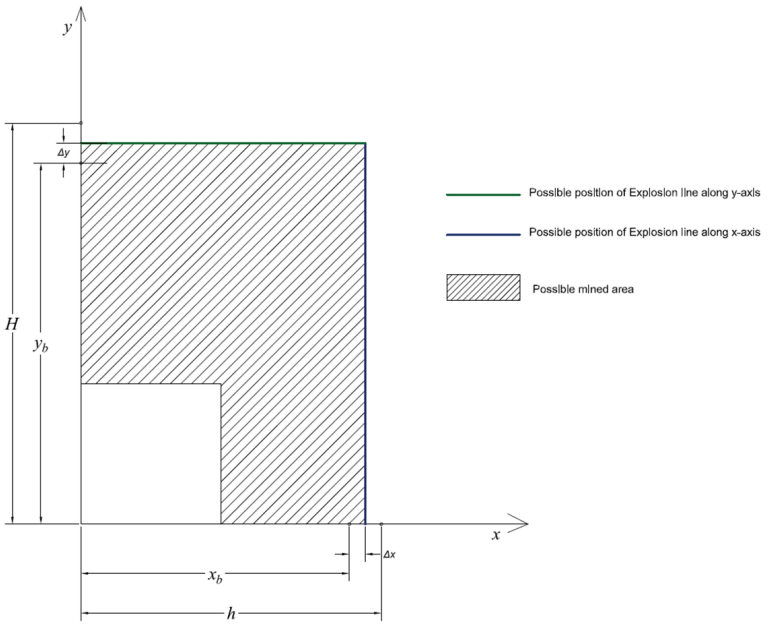


Figure 3. Graph of the one possible position along the x and y axes.

Finally, the uncertain value of criterion C2 expressed by Equation (24) is defined by the following equation:

$$O^u = \left(\left(x_b + N\left(\frac{x_b + h}{2},\ k \cdot (h - x_b) \right) \cdot \left(y_b + N\left(\frac{y_b + H}{2},\ k \cdot (H - y_b) \right) \right) - w_d \cdot h_d \right) \cdot b \cdot \gamma \tag{30}$$

The boundary of breaking rock from the mass is somewhere between y_b and H at the top and between x_b and h on the right side of the stope. A total of 500 simulations were conducted, and the results of each simulation were analyzed using the RAPS method to rank the alternatives. Finally, all rankings were aggregated, yielding a comprehensive final ranking and identifying the optimal solution.

The third criterion, C3, used for evaluating the proposed alternatives is the cost of drilling blastholes and explosives for each alternative. To support sustainability in small-scale underground mines, managing drilling and blasting costs is important for sustaining profitability, as these operations typically are a significant part of total expenses. Refining these costs requires finding a balance between maximizing efficiency and using resources appropriately, ensuring that mining activities stay both sustainable and economical. Based on this, the C3 criterion should be minimized. Cost depends on market conditions, namely the purchase price of explosives, drill fuel, consumables, labor, etc.

The time criterion, C4, for selecting the best blasting pattern in an underground mine refers to the duration of the drilling operation. This is especially important because reducing the time spent on these tasks leads to improved operational efficiency and greater overall productivity. Similar to the second criterion, this criterion can also be simulated to obtain more precise results, as it is difficult to maintain the same drilling time for each drillhole individually, let alone for the entire fan pattern. The uncertainty of this parameter depends on the different conditions of the working environment, equipment, operational conditions, labor force, etc. This is why simulation is used to describe uncertainty related to the duration of this activity, in simple terms, the drilling time. This is shown in the next equation:

$$T^u = t + \Delta t \tag{31}$$

where:

T^u—artificial value of time created by simulation, minutes,
t—calculated value needed for drilling one fan pattern not burdened by uncertainty, minutes.

Δt is governed by the normal distribution of the following form:

$$\Delta t \sim N(\mu, \sigma) \tag{32}$$

where:

μ—calculated value needed for drilling one fan pattern t,
σ—the standard deviation of the distribution that can be defined by the following equation:

$$\sigma = k \cdot (t) \tag{33}$$

where k is the coefficient, which takes the value of 0.1 or 10 percent of the calculated value. The value of the coefficient is adopted according to the experts' knowledge.

The fifth criterion, C5, for selecting the optimal blasting pattern is fragmentation. Poor fragmentation of blasted rock significantly impacts the costs associated with the later production stages following primary blasting. The desired fragmentation is determined by the equipment used for crushing the blasted material. The size of the rock fragments depends on factors, such as site characteristics, blasting design, and explosive power. In this context, it is difficult to precisely predict the size of the fragments. Therefore, the values used in the calculation are approximate estimates of the largest rock fragments resulting from the blasting process. It is also important to avoid oversized pieces to prevent the need for additional crashing, as this significantly affects production efficiency.

According to the criteria described above and the defined number of alternatives (nine) it is necessary to create a decision-making matrix with uncertainty. Uncertainty in the

decision-making matrix arises when values for criteria C2 and C4 are not crisp. For setting this task, it is necessary to create the decision-making matrix in the following manner:

$$M^u = \left[x_{ij}\right]^u_{9\times 5} = \begin{bmatrix} A/C & C_1 & C_2 & C_3 & C_4 & C_5 \\ A_1 & x_{11} & x_{12} \sim x^u_{12} & x_{13} & x_{14} \sim x^u_{14} & x_{15} \\ A_2 & x_{21} & x_{22} \sim x^u_{22} & x_{23} & x_{24} \sim x^u_{24} & x_{25} \\ A_3 & x_{31} & x_{32} \sim x^u_{32} & x_{33} & x_{34} \sim x^u_{34} & x_{35} \\ A_4 & x_{41} & x_{42} \sim x^u_{42} & x_{43} & x_{44} \sim x^u_{44} & x_{45} \\ A_5 & x_{51} & x_{52} \sim x^u_{52} & x_{53} & x_{54} \sim x^u_{54} & x_{55} \\ A_6 & x_{61} & x_{62} \sim x^u_{62} & x_{63} & x_{64} \sim x^u_{64} & x_{65} \\ A_7 & x_{71} & x_{72} \sim x^u_{72} & x_{73} & x_{74} \sim x^u_{74} & x_{75} \\ A_8 & x_{81} & x_{82} \sim x^u_{82} & x_{83} & x_{84} \sim x^u_{84} & x_{85} \\ A_9 & x_{91} & x_{92} \sim x^u_{92} & x_{93} & x_{94} \sim x^u_{94} & x_{95} \end{bmatrix} \tag{34}$$

For simulation s = 1, the uncertainty matrix is of the following form:

$$M^{s=1} = \left[x_{ij}\right]^{s=1}_{9\times 5} = \begin{bmatrix} A/C & C_1 & C_2 & C_3 & C_4 & C_5 \\ A_1 & x_{11} & x_{12} \sim x^{s=1}_{12} & x_{13} & x_{14} \sim x^{s=1}_{14} & x_{15} \\ A_2 & x_{21} & x_{22} \sim x^{s=1}_{22} & x_{23} & x_{24} \sim x^{s=1}_{24} & x_{25} \\ A_3 & x_{31} & x_{32} \sim x^{s=1}_{32} & x_{33} & x_{34} \sim x^{s=1}_{34} & x_{35} \\ A_4 & x_{41} & x_{42} \sim x^{s=1}_{42} & x_{43} & x_{44} \sim x^{s=1}_{44} & x_{45} \\ A_5 & x_{51} & x_{52} \sim x^{s=1}_{52} & x_{53} & x_{54} \sim x^{s=1}_{54} & x_{55} \\ A_6 & x_{61} & x_{62} \sim x^{s=1}_{62} & x_{63} & x_{64} \sim x^{s=1}_{64} & x_{65} \\ A_7 & x_{71} & x_{72} \sim x^{s=1}_{72} & x_{73} & x_{74} \sim x^{s=1}_{74} & x_{75} \\ A_8 & x_{81} & x_{82} \sim x^{s=1}_{82} & x_{83} & x_{84} \sim x^{s=1}_{84} & x_{85} \\ A_9 & x_{91} & x_{92} \sim x^{s=1}_{92} & x_{93} & x_{94} \sim x^{s=1}_{94} & x_{95} \end{bmatrix} \tag{35}$$

Applying the RAPS algorithm over matrix $M^{s=1} = \left[x_{ij}\right]^{s=1}_{9\times 5}$, the perimeter similarity vector is obtained:

$$PS^{s=1}_{i=9} = \begin{bmatrix} PS^{s=1}_1 \\ PS^{s=1}_2 \\ PS^{s=1}_3 \\ PS^{s=1}_4 \\ PS^{s=1}_5 \\ PS^{s=1}_6 \\ PS^{s=1}_7 \\ PS^{s=1}_8 \\ PS^{s=1}_9 \end{bmatrix} \tag{36}$$

According to the descending order of the obtained perimeter similarities, for s = 1, we get the rank of defined alternatives, which are presented by the vector:

$$R^{s=1}_{i=9} = \begin{bmatrix} A_1 & R_1 \in [1,2,\ldots,9] \\ A_2 & R_2 \in [1,2,\ldots,9] \\ A_3 & R_3 \in [1,2,\ldots,9] \\ A_4 & R_4 \in [1,2,\ldots,9] \\ A_5 & R_5 \in [1,2,\ldots,9] \\ A_6 & R_6 \in [1,2,\ldots,9] \\ A_7 & R_7 \in [1,2,\ldots,9] \\ A_8 & R_8 \in [1,2,\ldots,9] \\ A_9 & R_9 \in [1,2,\ldots,9] \end{bmatrix}^{s=1} \tag{37}$$

After a defined number of simulations s = 1, 2, . . ., S, we can create the total space of ranks in the following way:

$$R_{i=9}^{s=1,2,\ldots,\,S} = \begin{bmatrix} A_1 & R_1^{s=1} & R_1^{s=2} & \ldots & R_1^{s=S} \\ A_2 & R_2^{s=1} & R_2^{s=2} & \ldots & R_2^{s=S} \\ A_3 & R_3^{s=1} & R_3^{s=2} & \ldots & R_3^{s=S} \\ A_4 & R_4^{s=1} & R_4^{s=2} & \ldots & R_4^{s=S} \\ A_5 & R_5^{s=1} & R_5^{s=2} & \ldots & R_5^{s=S} \\ A_6 & R_6^{s=1} & R_6^{s=2} & \ldots & R_6^{s=S} \\ A_7 & R_7^{s=1} & R_7^{s=2} & \ldots & R_7^{s=S} \\ A_8 & R_8^{s=1} & R_8^{s=2} & \ldots & R_8^{s=S} \\ A_9 & R_9^{s=1} & R_9^{s=2} & \ldots & R_9^{s=S} \end{bmatrix} \quad (38)$$

The next step concerns summing up the elements of the ith row according to the equation:

$$R_i = \sum_{s=1}^{S} R_i^s \,,\ \forall\, i \in\ [1, 2, \ldots, 9] \quad (39)$$

Finally, the best alternative is defined by the following criteria:

$$A_{best} = min\left\{ \sum_{s=1}^{S} R_1^s \quad \sum_{s=1}^{S} R_2^s \quad \sum_{s=1}^{S} R_3^s \quad \ldots \quad \sum_{s=1}^{S} R_9^s \right\} \quad (40)$$

In Figure 4, the simulation process for n number of simulations is presented, showing the various stages and steps involved in running the simulation, including the input of initial data.

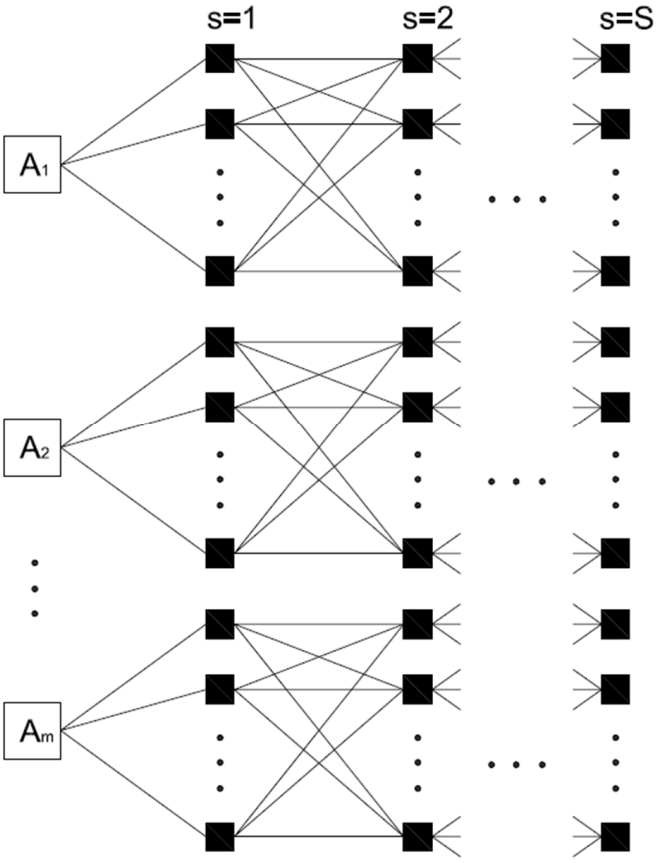


Figure 4. Simulation process.

3. Numerical Example

In this research, a hypothetical example of an underground mine is used to show the upgrade of the RAPS method with simulations, which are used because of uncertainty in some aspects of production. The numerical values applied in this study are based on real input data, in this case, data related to underground exploitation. This underground mine is considered a small-scale mine with an annual capacity of 100,000.00 tons of bauxite. The mining method that is used in this mine is called sublevel stoping. The selection of this method considered all relevant mining and geological parameters and exploitation conditions, as well as other technical and technological factors affecting extraction.

In this method, extraction is retreating, starting from the end of the production level and generally advancing toward the opening of the level, which is the transportation level. Bauxite extraction is conducted through fan drilling and blasting. The purpose of drilling blastholes is to allow the placement of explosives in the part of the rock mass that is planned for disintegration. It is important to emphasize that this is a small-scale mine, and such optimization plays a significant role in improving the mine's operations, particularly in terms of enhancing production efficiency and ensuring its long-term sustainability. Selecting suitable drilling and blasting parameters in small-scale mining is important for enhancing operational performance, lowering costs, and supporting safety. Proper planning of these operations is essential for reducing risks to worker safety and preserving the integrity of underground structures, which is particularly important in sensitive mining environments.

Blasthole drilling can either be semi-mechanized with manual hammers or fully mechanized using a range of drill rigs. Equipment that is available can provide the drilling of blastholes with a diameter range of Ø 41–45 mm. The bulk density of rock that is drilled is 2.54 $\frac{t}{m^3}$. For blasting, explosives in patrons are used. To obtain the finest possible bauxite, i.e., for as little dilution as possible, a 1-m-thick protective layer is left on the roof of the earlier work, which is not mined, temporarily keeping the waste rock from the old work.

Nine different fan patterns are calculated for this study. The height of the stope is one of parameters that is optimized. In this case, there are three different values of height that are entered into calculation. Another important parameter considered for optimization are the length of blastholes and burden. These two parameters affect the energy distribution from the explosives and the fragmentation size. Patterns and their geometrical parameters are shown in the next Table 1, and schemes of all proposed blasting patterns are shown in Figure 5.

Table 1. Parameters of fan patterns.

Alternatives	Total Length of Blastholes, m	Burden, m	Total Height of Stope, m
A1	21.8	1.5	8
A2	26.5	1.8	8
A3	29.5	2.0	8
A4	30.5	1.5	9
A5	33.7	1.8	9
A6	38.8	2.0	9
A7	38.5	1.5	10
A8	38.1	1.8	10
A9	44.1	2.0	10

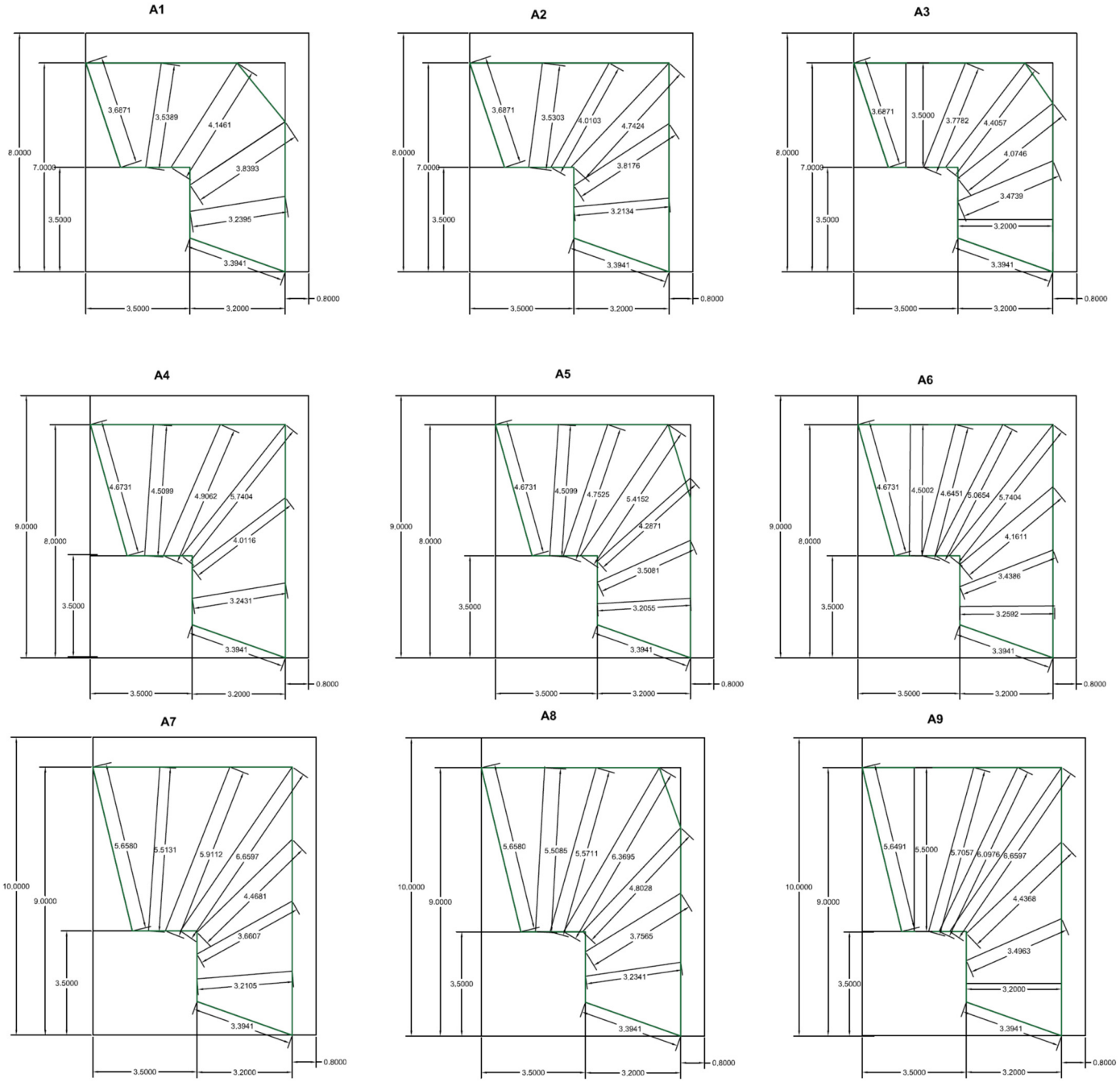


Figure 5. Schemes of proposed stope heights and fan patterns A1–A9 with corresponding geometry parameters.

The proper choice and coordination of all parameters are important for a successful mining operation. If any of these parameters are unsuitable or do not align with other geometric factors, the blast may result in poor fragmentation, environmental damage, or increased exploration costs. Therefore, it is necessary to ensure that all parameters are correctly aligned to keep a smooth and efficient exploitation process.

To achieve the desired aims in this example, five criteria have been selected to guide the process of choosing the best alternative. These criteria values for suggested alternatives are shown in the next Table 2. Values presented in the next table are calculated (ideal) values, without taking uncertainty into account.

Table 2. Calculated values of criteria for the selection of alternatives without uncertainty.

Alternative	Compactness Index	Tonnage, t	Cost, €/fan Pattern	Drilling Time (Minutes)	Fragmentation 1—Bad, 2—Medium, 3—Good
A1	4.46	151.02	650.00	106.35	2.00
A2	5.09	181.22	705.60	128.94	3.00
A3	4.45	201.36	774.00	141.02	1.00
A4	4.42	179.59	810.00	145.01	3.00
A5	3.98	215.51	834.00	157.98	1.00
A6	4.42	239.46	892.80	182.94	3.00
A7	4.15	208.17	954.00	176.97	2.00
A8	3.67	249.80	993.60	177.80	1.00
A9	4.15	277.56	1068.00	204.33	3.00

In Table 3, the input decision matrix is shown, with corresponding targets for each criterion, i.e., min or max target. Criteria C1, C3, and C5 are of deterministic values for each alternative, while C2 and C4 are burdened by uncertainty. The simulation of C2 is conducted, and 500 values for each alternative are created. It means that the total number of simulations is 500. Criterion C4 is obtained the same way. This criterion is simulated by the normal distribution with the mean value and corresponding standard deviation. The deviation is based on the expert's knowledge, and the value is 10% of the mean value.

Table 3. Input values for decision matrix, s = 1.

Criterion/ Alternative	C1	C2	C3	C4	C5
	min	max	min	min	max
A1	4.4559	166.0871	650.0000	109.3835	2.0000
A2	5.0858	205.7918	705.6000	136.2610	3.0000
A3	4.4475	219.1037	774.0000	152.8601	1.0000
A4	4.4155	193.1554	810.0000	164.3363	3.0000
A5	3.9803	208.7047	834.0000	175.8313	1.0000
A6	4.4180	231.1049	892.8000	172.7319	3.0000
A7	4.1500	204.8728	954.0000	192.7527	2.0000
A8	3.6724	238.9781	993.6000	177.7501	1.0000
A9	4.1482	290.1105	1068.0000	229.7601	3.0000

One possible simulation scenario of input data is presented in Table 3.

The next step of this method is normalization of the matrix shown in Table 3. The normalization process is conducted by applying Equations (2) and (3) depending on when the min or max criterion is involved. The normalized values of the above matrix are shown in Table 4.

After normalization of input data, the normalized matrix is weighted. As mentioned above, the standard deviation is used to assign the weights of criteria. This method also contributed to reducing subjectivity in this decision-making process. The obtained values of weights are shown in Table 5 and the diagram in Figure 6.

The next step in this process, shown in Table 6, is weighting the normalized matrix shown in Table 4.

Determining the optimal alternative by applying Equations (9) and (10) is the next step, and the result is shown in Table 7.

Table 4. Normalized matrix.

Criterion/ Alternative	C1	C2	C3	C4	C5
	min	max	min	min	max
A1	0.8242	0.5725	1.0000	1.0000	0.6667
A2	0.7221	0.7094	0.9212	0.8027	1.0000
A3	0.8257	0.7552	0.8398	0.7156	0.3333
A4	0.8317	0.6658	0.8025	0.6656	1.0000
A5	0.9227	0.7194	0.7794	0.6221	0.3333
A6	0.8312	0.7966	0.7280	0.6333	1.0000
A7	0.8849	0.7062	0.6813	0.5675	0.6667
A8	1.0000	0.8237	0.6542	0.6154	0.3333
A9	0.8853	1.0000	0.6086	0.4761	1.0000

Table 5. Weights of criteria obtained by applying the standard deviation.

Criterion/ Weight	C1	C2	C3	C4	C5
	w_1	w_2	w_3	w_4	w_5
W	0.0986	0.1517	0.1626	0.1928	0.3944

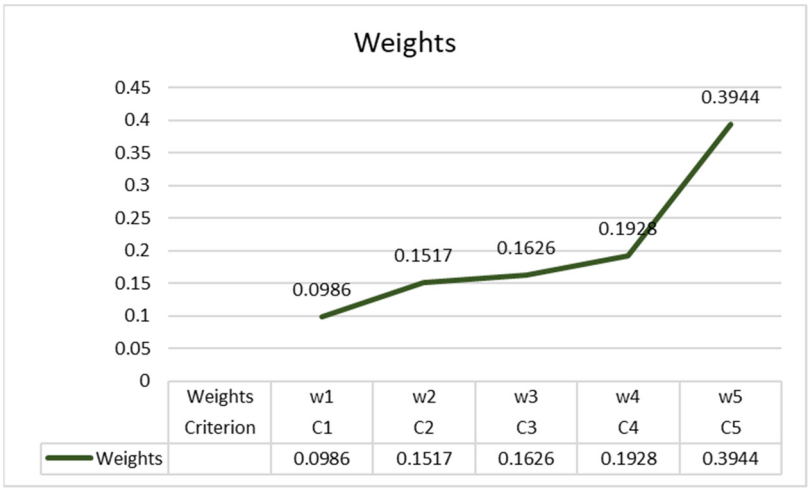


Figure 6. Graph of standard deviation-obtained weights.

Table 6. Weighting of the normalized matrix.

Criterion/ Alternative	C1	C2	C3	C4	C5
	min	max	min	min	max
A1	0.0813	0.0868	0.1626	0.1626	0.2629
A2	0.0712	0.1076	0.1497	0.1305	0.3944
A3	0.0814	0.1146	0.1365	0.1163	0.1315
A4	0.0820	0.1010	0.1304	0.1082	0.3944
A5	0.0910	0.1091	0.1267	0.1011	0.1315
A6	0.0820	0.1208	0.1183	0.1029	0.3944
A7	0.0873	0.1071	0.1108	0.0922	0.2629
A8	0.0986	0.1250	0.1063	0.1000	0.1315
A9	0.0873	0.1517	0.0989	0.0774	0.3944

Table 7. Optimal alternative.

Optimal Alternative/ Criterion	C1	C2	C3	C4	C5
	min	**max**	**min**	**min**	**max**
	q_1	q_2	q_3	q_4	q_5
Q	0.0986	0.1517	0.1626	0.1626	0.3944

Tables 8 and 9 present the decomposition of the optimal alternative and decomposition of all alternatives in this example.

Table 8. Decomposition of optimal alternatives.

Optimal Alternative/ Criterion	C1	C2	C3	C4	C5
	min	**max**	**min**	**min**	**max**
	q_1	q_2	q_3	q_4	q_5
Qmax		0.1517			0.3944
Qmin	0.0986		0.1626	0.1626	

Table 9. Decomposition of alternatives.

Criterion/ Alternative	C1	C2	C3	C4	C5
	min	**max**	**min**	**min**	**max**
	q_1	q_2	q_3	q_4	q_5
A1 Qmax		0.0868			0.2629
A1 Qmin	0.0813		0.1626	0.1626	
A2 Qmax		0.1076			0.3944
A2 Qmin	0.0712		0.1497	0.1305	
A3 Qmax		0.1146			0.1315
A3 Qmin	0.0814		0.1365	0.1163	
A4 Qmax		0.1010			0.3944
A4 Qmin	0.0820		0.1304	0.1082	
A5 Qmax		0.1091			0.1315
A5 Qmin	0.0910		0.1267	0.1011	
A6 Qmax		0.1208			0.3944
A6 Qmin	0.0820		0.1183	0.1029	
A7 Qmax		0.1071			0.2629
A7 Qmin	0.0873		0.1108	0.0922	
A8 Qmax		0.1250			0.1315
A8 Qmin	0.0986		0.1063	0.1000	
A9 Qmax		0.1517			0.3944
A9 Qmin	0.0873		0.0989	0.0774	

Table 9 represents the decomposition of each alternative for this process, which aims to obtain the best solution to our above-described problem.

By applying Equations (15) and (16), the next table is gained. Values in Table 10 represent the magnitude of the optimal alternative and other alternatives.

Table 10. Magnitude of the optimal alternative and each alternative.

	Max	**Min**
Optimal Alternative	**0.4225**	**0.2502**
A1	0.2769	0.2438
A2	0.4088	0.2110
A3	0.1744	0.1970
A4	0.4071	0.1883
A5	0.1708	0.1859
A6	0.4125	0.1770
A7	0.2839	0.1685
A8	0.1814	0.1762
A9	0.4225	0.1530

The final step of this process is to calculate the perimeter similarity of each alternative, that is presented in Table 11 and obtain the ranking according to the descending order. This step has been, as with all other steps, calculated 500 times, for each simulation.

Table 11. Perimeter similarity calculation of each alternative.

	Max	**Min**	**Perimeter**	**Perimeter Similarity**
	Q_k U_{ik}	Q_h U_{ih}	$P{=}Q_k{+}Q_h{+}\sqrt{Q_k^2{+}Q_k^2}$ $P_i{=}U_{ik}{+}U_{ih}{+}\sqrt{U_{ik}^2{+}U_{ih}^2}$	$PS_i{=}\frac{P_i}{P}, \forall i \in [1,2,\ldots,m]$
Q	0.4225	0.2502	1.1637	
A1	0.2769	0.2438	0.8897	0.7645
A2	0.4088	0.2110	1.0798	0.9279
A3	0.1744	0.1970	0.6344	0.5452
A4	0.4071	0.1883	1.0439	0.8970
A5	0.1708	0.1859	0.6092	0.5235
A6	0.4125	0.1770	1.0383	0.8922
A7	0.2839	0.1685	0.7825	0.6724
A8	0.1814	0.1762	0.6104	0.5245
A9	0.4225	0.1530	1.0249	0.8807

The final ranking of alternatives has been formed in descending order as the sum of all ranks for each alternative. The final rank and the optimal alternative are then presented.

Final ranking by the perimeter similarity of all alternatives is shown in the equation below. Summing of all ranks for each alternative in this simulation process is presented and shown in descending order. The smallest sum is the best alternative.

$$PS_{i=9}^{s=1} = \begin{bmatrix} PS_1^{s=1} = 0.7645 \\ PS_2^{s=1} = 0.9279 \\ PS_3^{s=1} = 0.5452 \\ PS_4^{s=1} = 0.8970 \\ PS_5^{s=1} = 0.5235 \\ PS_6^{s=1} = 0.8922 \\ PS_7^{s=1} = 0.6724 \\ PS_8^{s=1} = 0.5245 \\ PS_9^{s=1} = 0.8807 \end{bmatrix} \quad (41)$$

According to the descending order of the obtained perimeter similarities, for s = 1, we get the rank of defined alternatives, which are presented by the vector:

$$R_{i=9}^{s=1} = \begin{bmatrix} A_1 & R_1 = 5 \\ A_2 & R_2 = 1 \\ A_3 & R_3 = 7 \\ A_4 & R_4 = 2 \\ A_5 & R_5 = 9 \\ A_6 & R_6 = 3 \\ A_7 & R_7 = 6 \\ A_8 & R_8 = 8 \\ A_9 & R_9 = 4 \end{bmatrix}^{s=1} \tag{42}$$

Figure 7 illustrates the ranking of alternatives for s = 1.

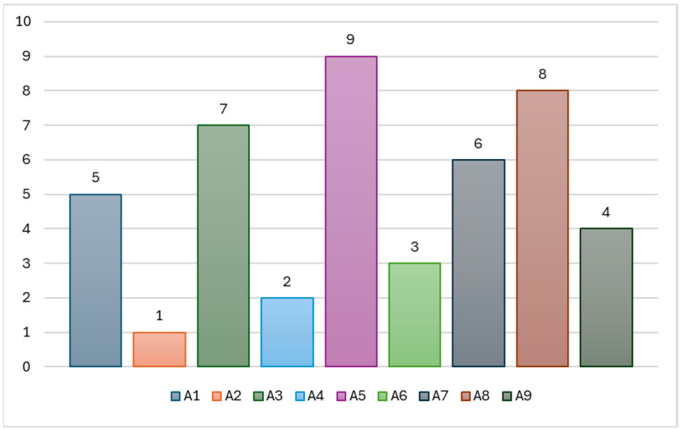


Figure 7. Ranking of alternatives for s = 1.

After defining the number of simulations s = 1, 2, . . ., 500, we can create the total space of ranks in the following way:

$$R_{i=9}^{s=1,2,\ldots,500} = \begin{bmatrix} A_1 & R_1^{s=1} & R_1^{s=2} & \ldots & R_1^{s=500} \\ A_2 & R_2^{s=1} & R_2^{s=2} & \ldots & R_2^{s=500} \\ A_3 & R_3^{s=1} & R_3^{s=2} & \ldots & R_3^{s=500} \\ A_4 & R_4^{s=1} & R_4^{s=2} & \ldots & R_4^{s=500} \\ A_5 & R_5^{s=1} & R_5^{s=2} & \ldots & R_5^{s=500} \\ A_6 & R_6^{s=1} & R_6^{s=2} & \ldots & R_6^{s=500} \\ A_7 & R_7^{s=1} & R_7^{s=2} & \ldots & R_7^{s=500} \\ A_8 & R_8^{s=1} & R_8^{s=2} & \ldots & R_8^{s=500} \\ A_9 & R_9^{s=1} & R_9^{s=2} & \ldots & R_9^{s=500} \end{bmatrix} \tag{43}$$

$$R_{i=9}^{s=1,2,\ldots,500} = \begin{bmatrix} A_1 & 5 & 5 & \ldots & 5 \\ A_2 & 1 & 2 & \ldots & 1 \\ A_3 & 7 & 8 & \ldots & 8 \\ A_4 & 2 & 1 & \ldots & 3 \\ A_5 & 9 & 7 & \ldots & 9 \\ A_6 & 3 & 4 & \ldots & 2 \\ A_7 & 6 & 6 & \ldots & 6 \\ A_8 & 8 & 9 & \ldots & 7 \\ A_9 & 4 & 3 & \ldots & 4 \end{bmatrix} \tag{44}$$

In Tables 12–14, the distribution of rankings of all alternatives for 100–500 simulations is shown.

Table 12. Distribution of rankings of all alternatives after 100 and 200 simulations.

	100 Simulations									200 Simulations								
	R1	**R2**	**R3**	**R4**	**R5**	**R6**	**R7**	**R8**	**R9**	**R1**	**R2**	**R3**	**R4**	**R5**	**R6**	**R7**	**R8**	**R9**
A1	0	0	0	0	100	0	0	0	0	0	0	0	0	200	0	0	0	0
A2	95	5	0	0	0	0	0	0	0	188	12	0	0	0	0	0	0	0
A3	0	0	0	0	0	0	53	28	19	0	0	0	0	0	0	102	56	42
A4	3	57	19	21	0	0	0	0	0	9	108	44	39	0	0	0	0	0
A5	0	0	0	0	0	0	18	33	49	0	0	0	0	0	0	41	68	91
A6	1	28	44	27	0	0	0	0	0	1	52	93	54	0	0	0	0	0
A7	0	0	0	0	0	100	0	0	0	0	0	0	0	0	200	0	0	0
A8	0	0	0	0	0	0	29	39	32	0	0	0	0	0	0	57	76	67
A9	1	10	37	52	0	0	0	0	0	2	28	63	107	0	0	0	0	0

Table 13. Distribution of rankings of all alternatives after 300 and 400 simulations.

	300 Simulations									400 Simulations								
	R1	**R2**	**R3**	**R4**	**R5**	**R6**	**R7**	**R8**	**R9**	**R1**	**R2**	**R3**	**R4**	**R5**	**R6**	**R7**	**R8**	**R9**
A1	0	0	0	0	300	0	0	0	0	0	0	0	0	400	0	0	0	0
A2	280	20	0	0	0	0	0	0	0	372	26	2	0	0	0	0	0	0
A3	0	0	0	0	0	0	154	88	58	0	0	0	0	0	0	204	115	81
A4	15	163	66	56	0	0	0	0	0	21	211	95	73	0	0	0	0	0
A5	0	0	0	0	0	0	65	114	121	0	0	0	0	0	0	87	157	156
A6	3	77	138	82	0	0	0	0	0	4	107	176	113	0	0	0	0	0
A7	0	0	0	0	0	300	0	0	0	0	0	0	0	0	400	0	0	0
A8	0	0	0	0	0	0	81	98	121	0	0	0	0	0	0	109	128	163
A9	2	40	96	162	0	0	0	0	0	3	56	127	214	0	0	0	0	0

Table 14. Distribution of rankings of all alternatives after 500 simulations.

	500 Simulations								
	R1	**R2**	**R3**	**R4**	**R5**	**R6**	**R7**	**R8**	**R9**
A1	0	0	0	0	500	0	0	0	0
A2	458	37	4	1	0	0	0	0	0
A3	0	0	0	0	0	0	250	149	101
A4	30	259	124	87	0	0	0	0	0
A5	0	0	0	0	0	0	118	186	196
A6	6	134	216	144	0	0	0	0	0
A7	0	0	0	0	0	500	0	0	0
A8	0	0	0	0	0	0	132	165	203
A9	6	70	156	268	0	0	0	0	0

Based on the distributions of ranking alternatives presented in Tables 12–14, it can be seen that similar results are achieved with 100 or more simulations. This consistency suggests that increasing the number of iterations is unlikely to lead to significantly different outcomes, affirming the robustness of the method used. In line with the aim of selecting the optimal alternative, Table 15 shows the percentage share of rankings for all alternatives if they appeared in first place, as the optimal solution.

Table 15. Percentage share of rankings R1 for every 100 simulations up to 500 for each alternative.

Percentage Share	100 Simulations	200 Simulations	300 Simulations	400 Simulations	500 Simulations
A1	0.00	0.00	0.00	0.00	0.00
A2	95.00	94.00	93.33	93.00	91.60
A3	0.00	0.00	0.00	0.00	0.00
A4	3.00	4.50	5.00	5.25	6.00
A5	0.00	0.00	0.00	0.00	0.00
A6	1.00	0.50	1.00	1.00	1.20
A7	0.00	0.00	0.00	0.00	0.00
A8	0.00	0.00	0.00	0.00	0.00
A9	1.00	1.00	0.67	0.75	1.20

In summing the elements of each row in Equation (44), we obtain the best alternative according to the following criteria:

$$A_{best} = min \quad \left\{ \sum_{s=1}^{S} R_1^s = 2500 \sum_{s=1}^{S} R_2^s = 548 \sum_{s=1}^{S} R_3^s = 3851 \sum_{s=1}^{S} R_4^s = 1268 \sum_{s=1}^{S} R_5^s = 4078 \sum_{s=1}^{S} R_6^s = 1498 \sum_{s=1}^{S} R_7^s = 3000 \sum_{s=1}^{S} R_8^s = 4071 \sum_{s=1}^{S} R_9^s = 1686 \right\} \tag{45}$$

Based on the obtained results of the sum of rankings for all evaluated alternatives, we can conclude that the best solution is the one with the lowest rank sum. In this case, alternative A2 has the lowest rank sum, making it the preferred choice. The second-best choice, based on the sum of rankings, would be alternative A4. On the other hand, the least favorable alternative in our numerical example is the alternative with the highest sum of ranks, which, in this case, is alternative A5. This shows that alternative A5 is the worst solution among the evaluated options. Figure 8 shows flow charts of the distribution of ranks for each alternative.

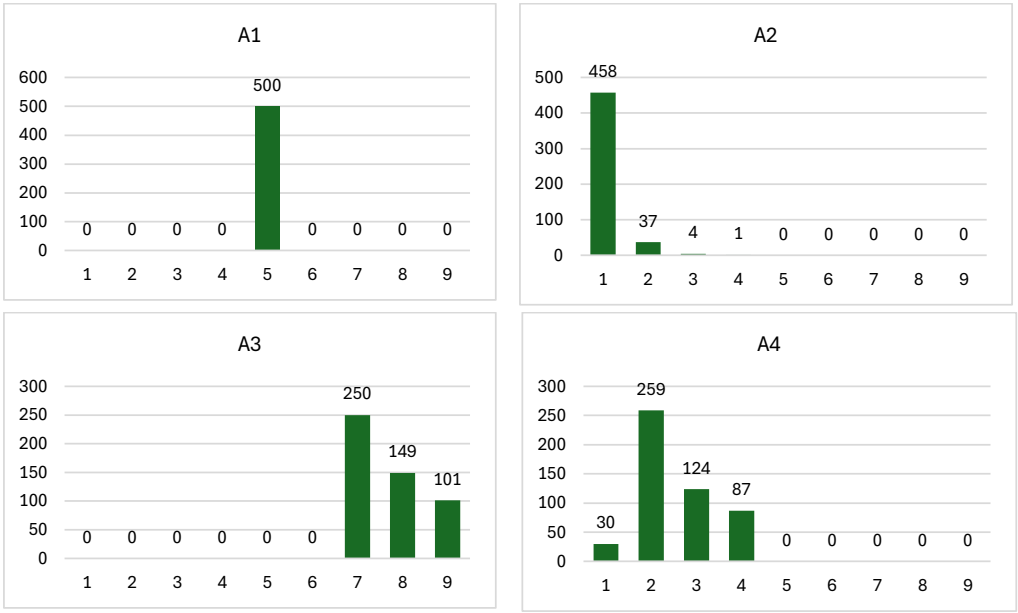


Figure 8. *Cont.*

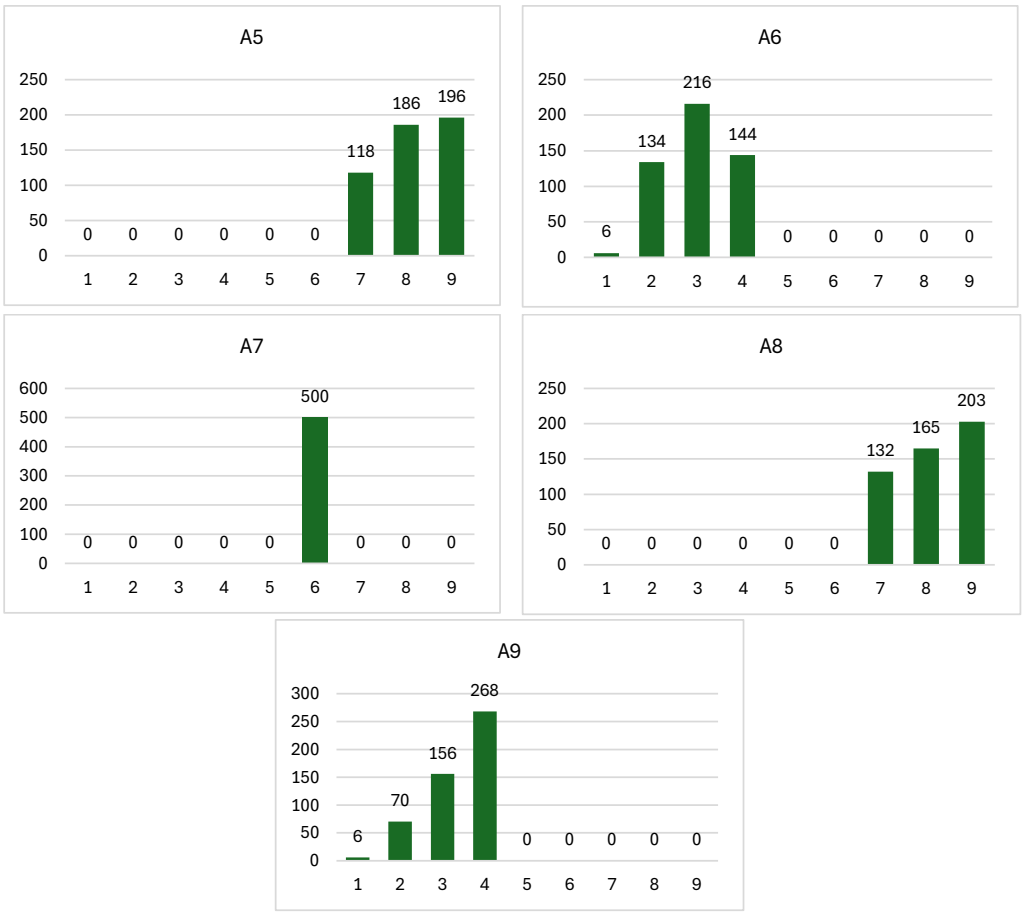


Figure 8. Distribution of ranks for each alternative A1–A9 (RAPS simulation method).

4. Validity Test of Simulation of the RAPS Method

The reliability and effectiveness of decision-making methods is important in improving complex processes. The validity of the RAPS method has been evaluated [21] using examples from research [26,27] using MCDM methods to evaluate 14 rooms according to 6 criteria for inside climate evaluation. The results of ranking rooms obtained with the RAPS method were compared with results obtained from other MCDM methods, and correlation coefficients are shown in Table 16.

Table 16. Correlation coefficients for different methods [21].

Correlation	RAPS	TAOV	ARAS	SAW	TOPSIS	COPRAS	VIKOR	WASPAS	ELECTRE
RAPS	-	0.89	0.95	0.88	0.96	0.96	0.80	0.95	0.78

In Table 16, the RAPS method shows a high degree of correlation with other MCDM methods. RAPS has the least correlation with ELECTRE. Three methods have a correlation coefficient between 0.80 and 0.89, while the other four have correlation coefficients with RAPS over 0.9 or higher.

To ensure the accuracy of the proposed methodology with numerical examples presented in this paper, a validity test was conducted using TOPSIS (technique for order preference by similarity to ideal solution combined with simulation) method.

For this validity test, we used the same input data as for the RAPS method. The simulation that is described above and implemented in the RAPS method is applied in the TOPSIS method to obtain the best solution for this decision-making process. After the application of TOPSIS on our numerical example, 500 ranks orders of alternatives are

obtained. These ranks are summed up and, in the same way as in our developed model, are ranked in ascending order. This is how the final rank is obtained. The next step in this test is the calculation of the correlation between our developed model and TOPSIS. The sum of rankings of alternatives by TOPSIS obtained after 500 simulations are:

$$A_{best} = min \left\{ \sum_{s=1}^{S} R_1^s = 2506 \sum_{s=1}^{S} R_2^s = 733 \sum_{s=1}^{S} R_3^s = 3743 \sum_{s=1}^{S} R_4^s = 1113 \sum_{s=1}^{S} R_5^s = 4093 \sum_{s=1}^{S} R_6^s = 1274 \sum_{s=1}^{S} R_7^s = 2992 \sum_{s=1}^{S} R_8^s = 4164 \sum_{s=1}^{S} R_9^s = 1882 \right\} \quad (46)$$

These rankings for each alternative individually are present in Figure 9.

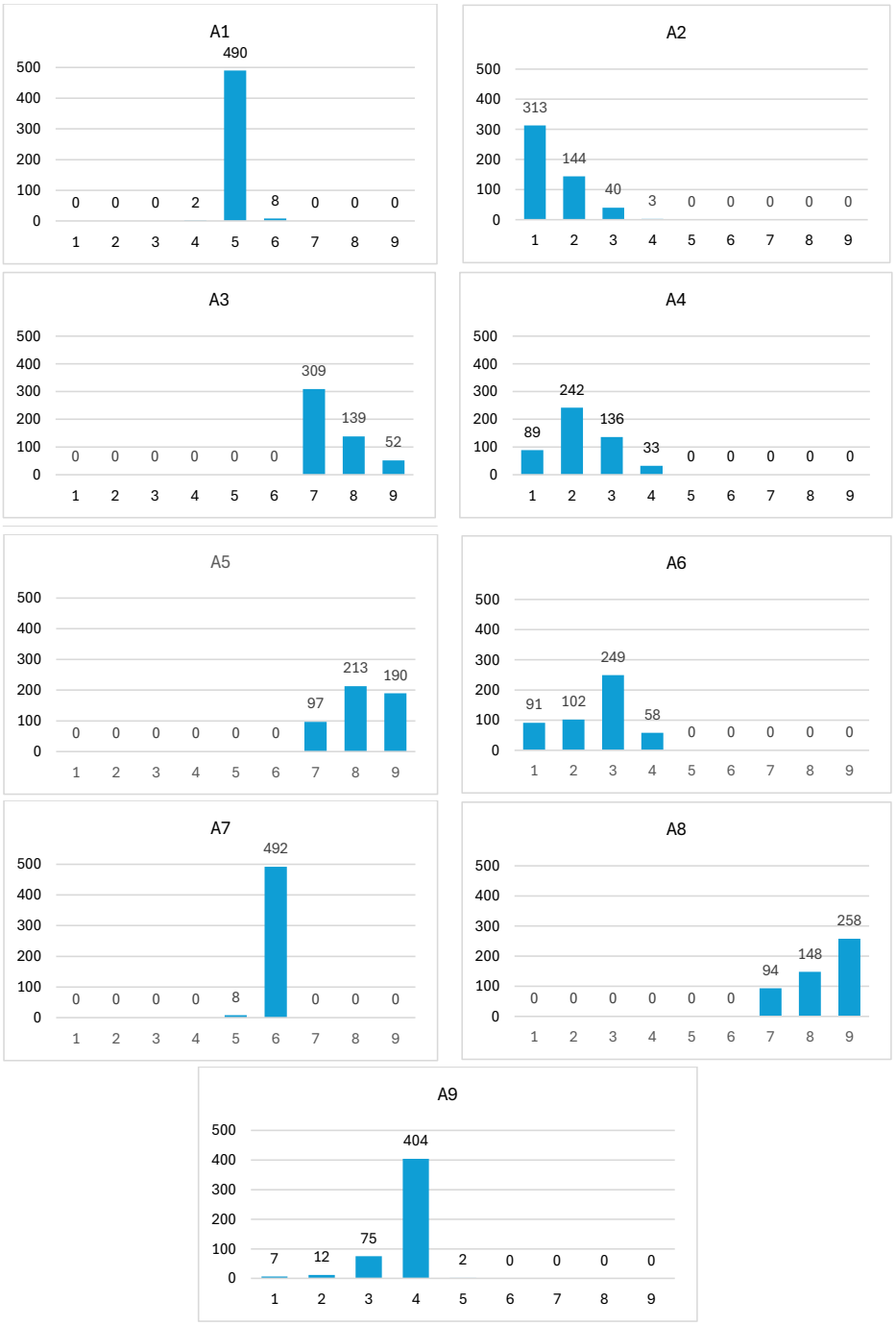


Figure 9. Flow charts of simulation-obtained rankings for each alternative A1–A9 (TOPSIS simulation method).

The results obtained by the TOPSIS simulation method, after 500 simulations, by summing all ranks of each alternative and sorting them in ascending order, show A2 as the optimal alternative, which is the same result obtained using our proposed methodology. The next best alternative according to the TOPSIS simulation method is A4, which also matches the second-best solution for our proposed methodology. The least adequate alternative according to the TOPSIS simulation method is A8, compared to our result, which is A5. The ranking results only differ in two positions of the alternatives when comparing both processes. A comparison of the results obtained from both methodologies is shown in Figure 10.

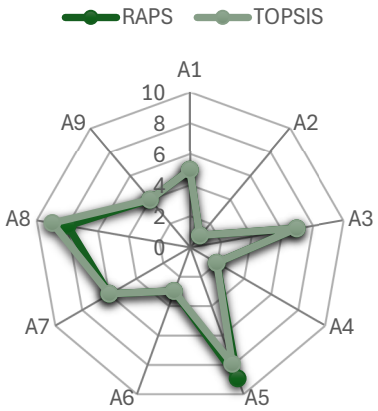


Figure 10. Comparative analysis of RAPS and TOPSIS final ranking.

After obtaining the results from these two methods combined with simulations, the correlation coefficient is calculated. Initially, this coefficient is calculated for each ranking order within every individual simulation. Once all individual coefficients are determined, the overall correlation coefficient is then calculated, providing a validation of the proposed model with the well-known TOPSIS method.

The accuracy parameter based on Pearson's [28] coefficient of correlation can be used to check the validity of the proposed methodology.

The expected value of the correlation coefficient between RAPS simulation and TOPSIS simulation is 0.9833. The correlation between RAPS and TOPSIS, according to Selvanathan et al. [29], belongs to the "very high correlation". The distribution of coefficients of correlation of each simulation for RAPS and TOPSIS is shown in the histogram in Figure 11.

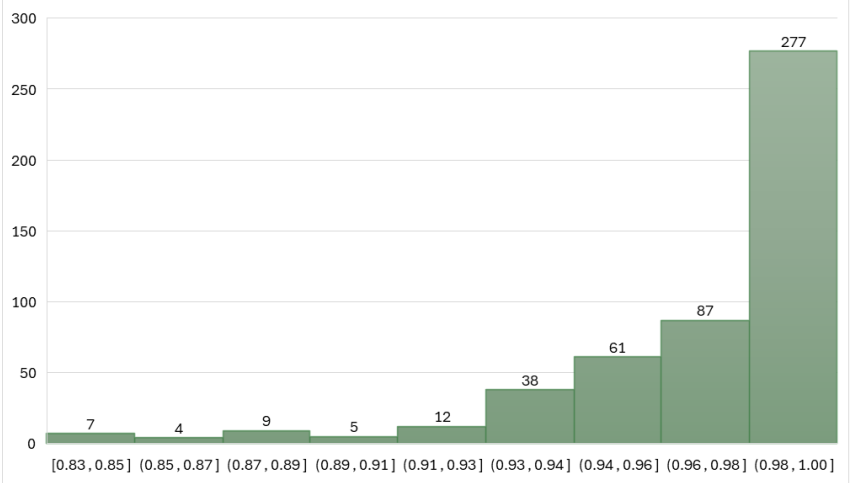


Figure 11. Histogram of correlation coefficients for all 500 simulations.

5. Discussion

In this paper, the RAPS method is employed for selecting optimal solutions in addressing the challenges of a presented underground mine problem. Simulation is proposed to apply to some of the criteria that are not rigid or deterministic, meaning these criteria do not have a fixed value. In this numerical example, two criteria are more accurately represented through simulation. This modification of ranking alternatives by perimeter similarity makes the method more flexible and more convenient for facing uncertainty in the decision-making process.

This paper demonstrated how to optimize stope production in a small-scale underground mine where bauxite is being extracted. In small-scale mines like this one, it is very important to improve the mine's operations, particularly in enhancing production efficiency and, in that way, ensuring long-term sustainability.

For this hypothetical example, with an annual capacity of 100,000.00 tons of bauxite, nine different fan patterns are proposed, with three different stope heights and burden from which to select. Drilling and blasting represent very important operations for production in most of the mines because their purpose is to separate ore from the rock mass. The appropriate selection of all parameters is crucial for a successful mining operation. If any parameter is unsuitable with other geometric factors, the blast may lead to poor fragmentation, environmental issues, or higher exploration costs. Therefore, ensuring proper selection of all parameters is essential for maintaining an efficient extraction process.

After defining alternatives, five criteria important to this evaluation process were chosen. Criteria selected as adequate for this process are the compactness index of fan pattern, tonnage gathered from one blasting, cost of each pattern, drilling time for total length of the blastholes in each alternative, and fragmentation of mined ore. Every criterion is important for a specific aspect of ore extraction and should be given a very high level of attention.

The presence of uncertainty in this process has led us to develop an appropriate methodology to carry out the decision-making process in the most efficient way possible. Two criteria (C2 and C4) were simulated and combined with steps of the RAPS method, to rank the alternatives. The simulation process was conducted 500 times, and therefore, we obtained 500 rankings for each alternative. Summing up the results of the ranking for each alternative and after arranging all those sums in ascending order, the final rank is obtained.

To validate our proposed methodology, we applied the TOPSIS method to the same numerical example with simulation of the same criteria (C2 and C4). The results were obtained the same way as in the RAPS method; first, 500 rankings of each alternative are summed and then arranged in ascending order to obtain the final ranking. These results show A2 as the optimal alternative, which is the same result obtained using our proposed methodology. The next best alternative according to the TOPSIS simulation method is A4, which also matches the second-best solution of our proposed methodology. The least adequate alternative according to the TOPSIS simulation method is A8, compared to our result, which is A5. The ranking results only differs in two positions of the alternatives when comparing both processes.

The results of comparative analyses between the results of RAPS simulation and TOPSIS simulation, described by the linguistic variables, have shown that correlation is "very high". The stability of the proposed methodology is evident, and with a correlation coefficient of 0.9833, it can be confirmed that this approach is applicable to the described mining problem.

6. Conclusions

This research involved an MCDM method to evaluate and prioritize options when there are multiple factors to consider. When making decisions under uncertainty, such as optimizing the stope and fan pattern in underground mining, especially small-scale mines like the one presented in this research, it is important to consider both economic and production factors. This paper demonstrated the use of simulations combined with the RAPS method for stope and fan pattern selection in an underground bauxite mine.

In the previous part of this research, nine different fan patterns were proposed. For each of them, five criteria were determined. After simulating two criteria and implementing them in the RAPS method along with the other three criteria with fixed values, the optimal alternative is selected. As the optimal alternative, after summing all rankings, A2 is selected in this example. This alternative has a total length of blastholes of 26.5 m, burden of 1.8 m, and height of the stope of 8 m, making it an ideal fan pattern for this bauxite production in an underground mine. The proposed methodology is stable, and with a correlation coefficient of 0.9833, it can be concluded that this methodology is applicable to our mining problem.

The proposed algorithm is developed using Microsoft Excel, keeping in mind that most mining engineers already use Excel daily. This familiarity with Excel allows for seamless integration of the developed method into their routine workflows.

The model is not closed and can be expanded to include a component that considers the human factor. This would involve conducting specific surveys whose results would be processed and integrated into the decision-making system, enabling a more holistic approach to data analysis. The proposed methodology is not limited in its application; it can be utilized in a wide variety of mining locations and mining-related problems where selecting the best solution among multiple alternatives is required.

Further research could focus on the fuzzification process of input parameters according to their nature. Another approach for treating the uncertainty of input data could involve introducing grey-interval numbers in the decision-making process. To enhance the accuracy in selecting the optimal solution, particularly when choosing production parameters for the stope related to fan drilling and blasting, as in a previous example, the number of criteria influencing the decision could be expanded. In subsequent research, additional criteria related to operational costs could be included, such as the costs of transporting ore from the excavation site, ventilation costs, and investments in transportation and ventilation equipment. All these costs are dependent on the quantities of ore extracted.

Author Contributions: Conceptualization, K.U. and Z.G.; methodology, K.U.; validation, B.G. and Z.G.; formal analysis, Č.B. and I.J.; writing original draft preparation, K.U.; supervision, Č.B. All authors have read and agreed to the published version of the manuscript.

Funding: This research received no external funding.

Data Availability Statement: The original contributions presented in this study are included in the article. Further inquiries can be directed to the corresponding author.

Acknowledgments: The research presented in this paper was conducted with the support of the Ministry of Science, Technology, and Innovation of the Republic of Serbia, within the framework of support for scientific research at the University of Belgrade, Faculty of Mining and Geology in Belgrade, under contract number 451-03-65/2024-03/200126.

Conflicts of Interest: The authors declare no conflicts of interest.

Abbreviations

The following abbreviations are used in this manuscript:

MCDM	Multiple Criteria Decision Making
RAPS	Ranking Alternatives by Perimeter Similarity
TOPSIS	Technique for Order of Preference by Similarity to Ideal Solution
AHP	Analytic Hierarchy Process
PROMETHEE	Preference Ranking Organization Method for Enrichment of Evaluations
ELECTRE	Elimination Et Choice Translating Reality
TAOV	Total Area Based on Orthogonal Vectors
ARAS	Additive Ratio Assessment
WASPAS	Weighted Aggregated Sum Product Assessment
COPRAS	Complex Proportional Assessment

References

1. Sitorus, F.; Cilliers, J.J.; Brito-Parada, P.R. Multi-criteria decision making for the choice problem in mining and mineral processing: Applications and trends. *Expert Syst. Appl.* **2019**, *121*, 393–417. [CrossRef]
2. Brans, J.P.; Vincke, P.; Mareschal, B. How to select and how to rank projects: The PROMETHEE method. *Eur. J. Oper. Res.* **1986**, *24*, 228–238. [CrossRef]
3. Roy, B. The outranking approach and the foundations of ELECTRE methods. In *Readings in Multiple Criteria Decision Aid*; Springer: Berlin/Heidelberg, Germany, 1990; pp. 155–183.
4. Saaty, T.L. *The Analytic Hierarchy Process*; McGraw-Hill: New York, NY, USA, 1980.
5. Tzeng, G.H.; Huang, J.J. *Multiple Attribute Decision Making: Methods and Applications*; CRC Press: Boca Raton, FL, USA, 2011.
6. Pouresmaieli, M.; Ataei, M.; Nouri Qarahasanlou, A.; Barabadi, A. Multi-criteria Decision-making Methods for Sustainable Decision-making in the Mining Industry (A Comprehensive Study). *J. Min. Environ.* **2024**, *15*, 683–706.
7. Himanshu, V.K.; Mishra, A.K.; Roy, M.P.; Singh, P.K. Underground Ring Blasting. In *Blasting Technology for Underground Hard Rock Mining*; Springer Nature: Singapore, 2023; pp. 75–91.
8. Namin, F.S.; Ghadi, A.; Saki, F. A literature review of Multi Criteria Decision-Making (MCDM) towards mining method selection (MMS). *Resour. Policy* **2022**, *77*, 102676. [CrossRef]
9. Bakhtavar, E.; Yousefi, S.; Jafarpour, A. Evaluation of shaft locations in underground mines: Fuzzy multi-objective optimization by ratio analysis with fuzzy cognitive map weights. *J. South. Afr. Inst. Min. Metall.* **2019**, *119*, 855–864. [CrossRef] [PubMed]
10. Cardozo, F.A.; Campos, H.J.; Petter, C.O.; Ambrós, W.M. Application of Monte Carlo Analytic Hierarchy Process (MAHP) in Underground Mining Access Selection. *Mining* **2023**, *3*, 773–785. [CrossRef]
11. Rahimdel, M.J.; Aryafar, A.; Tavakkoli, E. Selection of the most proper drilling and blasting pattern by using MADM methods (A case study: Sangan Iron Ore Mine, Iran). *Rud.-Geološko-Naft. Zb.* **2020**, *35*. [CrossRef]
12. Sandanayake DS, S.; Topal, E.; Asad MW, A. Designing an optimal stope layout for underground mining based on a heuristic algorithm. *Int. J. Min. Sci. Technol.* **2015**, *25*, 767–772. [CrossRef]
13. Li, C.; Liu, G.; Guo, L.; Zheng, D.; Yuan, X. A New CRITIC-GRA Model for Stope Dimension Optimization Considering Open Stoping Stability, Mining Capacity and Costs. *Appl. Sci.* **2024**, *14*, 5249. [CrossRef]
14. Qiu, H.-Y.; Huang, M.-Q.; Weng, Y.-J. Stability Evaluation and Structural Parameters Optimization of Stope Based on Area Bearing Theory. *Minerals* **2022**, *12*, 808. [CrossRef]
15. Onederra, I.; Chitombo, G. Design methodology for underground ring blasting. *Min. Technol.* **2007**, *116*, 180–195. [CrossRef]
16. Wang, M.; Shi, X.; Zhou, J. Charge design scheme optimization for ring blasting based on the developed Scaled Heelan model. *Int. J. Rock Mech. Min. Sci.* **2018**, *110*, 199–209. [CrossRef]
17. Blair, D.P.; Minchinton, A. Near-field blast vibration models. In Proceedings of the 8th International Symposium of Rock Fragmentation by Blasting, Santiago, Chile, 7–11 May 2006; pp. 152–159.
18. Bai, X.; Marcotte, D.; Simon, R. Underground stope optimization with network flow method. *Comput. Geosci.* **2013**, *52*, 361–371. [CrossRef]
19. Vishwakarma, A.K.; Dey, K.; Himanshu, V.K.; Singh, R.K.; Roy, M.P. Optimization of Blast Design Parameter for Ring Blasting in Underground Hard Rock Mine Using Numerical Simulation. *Min. Metall. Explor.* **2024**, *41*, 139–148. [CrossRef]
20. Vishwakarma, A.K.; Himanshu, V.K.; Dey, K. Determination of Optimal Burden for Ringhole Blasting in Underground Hard Rock Mining Under Varying Geotechnical Properties. *Rock Mech. Rock Eng.* **2024**, *57*, 5727–5741. [CrossRef]
21. Urošević, K.; Gligorić, Z.; Miljanović, I.; Beljić, Č.; Gligorić, M. Novel Methods in Multiple Criteria Decision-Making Process (MCRAT and RAPS)—Application in the Mining Industry. *Mathematics* **2021**, *9*, 1980. [CrossRef]
22. Schwartzberg, J.E. Reapportionment, gerrymanders, and the notion of compactness. *Minn. Law Rev.* **1966**, *50*, 443–452.

23. Baker, W.E.; Cox, P.A.; Kulesz, J.J.; Strehlow, R.A.; Westine, P.S. *Explosion Hazards and Evaluation*; Elsevier Scientific Pub. Co., Ltd.: Amsterdam, The Netherlands, 1983.
24. Zhang, Z.-X.; Sanchidrián, J.A.; Ouchterlony, F.; Luukkanen, S. Reduction of fragment size from mining to mineral processing: A review. *Rock Mech. Rock Eng.* **2023**, *56*, 747–778. [CrossRef]
25. Zardari, N.H.; Ahmed, K.; Shirazi, S.M.; Yusop, Z.B. *Weighting Methods and Their Effects on Multi-Criteria Decision Making Model Outcomes in Water Resources Management*; Springer: Cham, Switzerland, 2014.
26. Hajiagha, S.H.R.; Mahdiraji, H.A.; Hashemi, S.S. Total area based on orthogonal vectors (Taov) as a novel method of multi-criteria decision aid. *Technol. Econ. Dev. Econ.* **2018**, *24*, 1679–1694. [CrossRef]
27. Zavadskas, E.K.; Turskis, Z. A new additive ratio assessment (ARAS) method in multicriteria decision-making. *Technol. Econ. Dev. Econ.* **2010**, *16*, 159–172. [CrossRef]
28. Benesty, J.; Chen, J.; Huang, Y.; Cohen, I. Pearson Correlation Coefficient. In *Noise Reduction in Speech Processing. Springer Topics in Signal Processing*, 2nd ed.; Springer: Berlin/Heidelberg, Germany, 2009.
29. Selvanathan, M.; Jayabalan, N.; Saini, G.K.; Supramaniam, M.; Hussin, N. Employee productivity in Malaysian private higher educational institutions. *PalArch's J. Archaeol. Egypt/Egyptol.* **2020**, *17*, 66–79.

Disclaimer/Publisher's Note: The statements, opinions and data contained in all publications are solely those of the individual author(s) and contributor(s) and not of MDPI and/or the editor(s). MDPI and/or the editor(s) disclaim responsibility for any injury to people or property resulting from any ideas, methods, instructions or products referred to in the content.